



HAL
open science

Predictive Value of Cellular Accumulation of Hydrophobic Bile Acids as a Marker of Cholestatic Drug Potential

Audrey Burban, Ahmad Sharaneek, Lydie Humbert, Thibaut Eguether, Christiane Guguen-Guillouzo, Dominique Rainteau, André Guillouzo

► **To cite this version:**

Audrey Burban, Ahmad Sharaneek, Lydie Humbert, Thibaut Eguether, Christiane Guguen-Guillouzo, et al.. Predictive Value of Cellular Accumulation of Hydrophobic Bile Acids as a Marker of Cholestatic Drug Potential. *Toxicological Sciences*, 2019, 168 (2), pp.474-485. 10.1093/toxsci/kfz009 . hal-02020472

HAL Id: hal-02020472

<https://univ-rennes.hal.science/hal-02020472>

Submitted on 13 Mar 2019

HAL is a multi-disciplinary open access archive for the deposit and dissemination of scientific research documents, whether they are published or not. The documents may come from teaching and research institutions in France or abroad, or from public or private research centers.

L'archive ouverte pluridisciplinaire **HAL**, est destinée au dépôt et à la diffusion de documents scientifiques de niveau recherche, publiés ou non, émanant des établissements d'enseignement et de recherche français ou étrangers, des laboratoires publics ou privés.

PREDICTIVE VALUE OF CELLULAR ACCUMULATION OF HYDROPHOBIC BILE ACIDS AS A MARKER OF CHOLESTATIC DRUG POTENTIAL

Audrey BURBAN^{1,2*}, Ahmad SHARANEK^{1,2*}, Lydie HUMBERT³, Thibaut EGUETHER³,
Christiane GUGUEN-GUILLOUZO^{1,2}, Dominique RAINTEAU³ and André GUILLOUZO^{1,2}

* Both authors contributed equally to this work

¹INSERM U1241, Numecan, Rennes

²University of Rennes 1, Rennes, France

³ERL INSERM U1157/UMR7203, Faculty of Medicine Pierre et Marie Curie Saint Antoine,
Paris, France

Address correspondence to: André Guillouzo, Inserm UMR 1241, Faculté des Sciences
Pharmaceutiques et Biologiques, 35043 Rennes Cedex, France. Email:
andre.guillouzo@univ-rennes1.fr

Key words: HepaRG hepatocytes; hydrophobic bile acids; cholestatic drugs;
noncholestatic drugs; lithocholic acid; sulfation; amidation

Abstract

Drug-induced cholestasis is mostly intrahepatic and characterized by alterations of bile canaliculi dynamics and morphology as well as accumulation of bile acids (BAs) in hepatocytes. However, little information exists on first changes in BA content and profile induced by cholestatic drugs in human liver. In the present study we aimed to analyze the effects of a large set of cholestatic and noncholestatic drugs in presence of physiological serum concentrations and 60-fold higher levels of 9 main BAs on cellular accumulation of BAs using HepaRG hepatocytes. BAs were measured in cell layers (cells + bile canaliculi) and culture media using HPLC coupled with tandem MS/MS after 24h-treatment. Comparable changes in total and individual BA levels were observed in cell layers and media from control and noncholestatic drug-treated cultures: unconjugated BAs were actively amidated and lithocholic acid (LCA) was entirely sulfated. By contrast, cellular accumulation of LCA and in addition, of the two other hydrophobic BAs, chenodeoxycholic acid and deoxycholic acid, was evidenced only with cholestatic compounds in presence of BA mixtures at normal and 60-fold serum levels, respectively, suggesting that LCA was the first BA to accumulate. Cellular accumulation of hydrophobic BAs was associated with inhibition of their amidation and for LCA, its sulfation. In conclusion, these results demonstrated that cellular accumulation of unconjugated hydrophobic BAs can be caused by various cholestatic drugs in human hepatocytes and suggest that their cellular detection, especially that of LCA, could represent a new strategy for evaluation of cholestatic potential of drugs and other chemicals.

Introduction

Cholestasis is typified by accumulation of bile acids (BAs) or their conjugated bile salts in the liver and systemic circulation. Both intrahepatic and extrahepatic cholestasis of various etiologies have been described in humans; they may be due to impaired secretion of BAs by hepatocytes or obstruction of either intrahepatic or extrahepatic bile ducts. Accumulation of pigmented material in hepatocytes and the lumen of bile canaliculi (BCs) and some irregularly dilated BCs with conspicuous alterations of microvilli have been visualized in cholestatic liver (Layden *et al.*, 1975).

Cholestasis is associated with an increase in serum BA content that can reach 60-fold or more normal values as well as major changes in their profiles (Humbert *et al.*, 2012; Trottier *et al.*, 2012). An increase in serum BA conjugates has been observed in intrahepatic cholestasis of pregnancy (Castano *et al.*, 2006; Reyes *et al.*, 2000; Tribe *et al.*, 2010), obstructive cholestasis (Woolbright *et al.*, 2015) and in infants with biliary atresia (Abukawa *et al.*, 1998). By contrast, BA content is decreased in bile compared to normal values but is still much higher than in serum in cholestatic patients (Humbert, *et al.*, 2012; Woolbright, *et al.*, 2015). Secondary hydrophobic unconjugated BAs are decreased in serum of cholestatic patients versus healthy subjects (Humbert, *et al.*, 2012).

Data on total content and profile of BAs in normal and cholestatic human liver are scarce compared to those in serum and bile (Garcia-Canaveras *et al.*, 2012). A marked increase in total and unconjugated BAs has been found in the liver of young infants with biliary atresia (Abukawa, *et al.*, 1998) and in chronic cholestatic liver disease (Fischer *et al.*, 1996).

Primary BAs, namely cholic acid (CA) and chenodeoxycholic acid (CDCA), are synthesized in hepatocytes from cholesterol by two multistep pathways. They are then conjugated to glycine or taurine, giving rise to taurocholic acid (TCA), glycocholic acid (GCA), glycochenodeoxycholic acid (GCDCA), and taurochenodeoxycholic acid (TCDCA). These conjugated (amidated) BAs may also be metabolized by different liver enzymes such as cytochrome P450s, and glucuronosyl- and sulfo-transferases (Chiang, 2009). After secretion into bile via canalicular transporters, mainly the bile salt efflux pump (BSEP), conjugated BAs

are released into the duodenum, where they facilitate the absorption of dietary lipids and liposoluble vitamins. The gut microbiota catalyzes 7 α -dehydroxylation of CDCA and CA to generate the secondary BAs, namely lithocholic (LCA) and deoxycholic (DCA) acids (Monte *et al.*, 2009). Around 95% of both primary and secondary BAs can be reabsorbed and return back to the liver *via* the enterohepatic circulation (Anwer, 2014; Chiang, 2009).

Many drugs can induce intrahepatic and more rarely extrahepatic cholestasis in a minority of patients. As in cholestasis of other etiologies changes in total BAs and profiles have been reported in both serum and bile of patients suffering from drug-induced cholestasis. By contrast, there is little information on early changes in BA total content and profile in human liver exposed to cholestatic drugs. Indeed, the first steps cannot be analyzed in humans and differences in BA synthesis, regulation and composition with animals limit the interest of these latter (Chiang, 2009). In support, many drugs can cause cholestasis in humans without inducing any significant liver injury in preclinical animal models (Fattinger *et al.*, 2001). An increase in hydrophobic BAs, i.e. CDCA, LCA and DCA, is thought to cause liver injury (Woolbright, et al., 2015). However, molecular mechanisms by which BAs induce liver injury remain poorly elucidated.

BC dynamics are impaired during cholestasis; this alteration is associated with disruption of the Rho/Myosin light chain kinases (ROCK/MLCK) signaling pathway, actin cytoskeleton rearrangement, BC deformations and cellular accumulation of BAs (Sharanek *et al.*, 2016; Sharanek *et al.*, 2017). Several molecular targets of the tested cholestatic compounds have been identified in the ROCK/MLCK pathway (Burban *et al.*, 2018; Burban *et al.*, 2017; Sharanek, et al., 2016). Recently, we reported that in presence of physiological serum BA concentrations, three major cholestasis drugs, namely cyclosporine A (CsA), chlorpromazine (CPZ) and troglitazone (TRO), induced preferential cellular accumulation of the three major hydrophobic BAs, i.e. lithocholic, deoxycholic and chenodeoxycholic acids, in their unconjugated forms, using differentiated HepaRG cells. Importantly, these three drugs can cause irreversible constriction while many other cholestatic drugs are causing dilatation of BCs (Antherieu *et al.*, 2013; Burban, et al., 2018; Burban, et al., 2017; Burbank *et al.*, 2016;

Sharanek, et al., 2016), leading to question whether rapid intracellular accumulation of hydrophobic BAs is a general feature induced by cholestatic drugs. In the current study, using a large set of cholestatic and noncholestatic compounds, we show that only cholestatic drugs caused cellular accumulation of hydrophobic BAs after a short treatment in the presence of exogenous BAs.

Materials and Methods

Reagents

Flucloxacillin (FLX), levofloxacin (LVX), erythromycin (ERY), ampicillin (AMP), streptomycin (SM), perhexiline (PER), troglitazone (TRO), amiodarone (AMI), acetaminophen (APAP) and methylthiazoletetrazolium (MTT) were purchased from Sigma (St. Quentin Fallavier, France). Macitentan (MAC) and sitaxentan (SIT) were provided by Alsachim (St. Illkirch-Graffenstaden, France). Bosentan (BOS) was obtained from Sequoia Research Products (Pangbourne, U.K). Fasudil (FAS) (HA-1077) was from BPS Bioscience (Le Perray en Yvelines, France). Ambrisentan (AMB) was a gift from MSN Laboratories (Sanath Nagar, India). Other chemicals were of reagent grade.

HepaRG cell cultures and treatments

All HepaRG cell cultures were prepared from vials of the same frozen cell badge and incubated with the same HyClone fetal calf serum. Before starting the treatments HepaRG cells were differentiated as previously described (Cerec *et al.*, 2007). Briefly, cells were seeded at a density of 2.6×10^4 cells/cm² in Williams' E medium supplemented with 2 mM glutamax, 100 U/mL penicillin, 100 µg/mL streptomycin, 10% HyClone fetal calf serum, 5 µg/mL insulin, and 50 µM hydrocortisone hemisuccinate. After 2 weeks they were shifted to the same medium supplemented with 1.7% dimethyl sulfoxide (DMSO) for 2 additional weeks to obtain confluent differentiated cultures containing around equal proportions of hepatocyte-like and progenitor/primitive biliary-like cells. For measurement of BAs cultures were prepared in 10 cm petri dishes. The medium was supplemented with 2% fetal bovine

charcoal-stripped serum (BA-free serum) (Sigma, reference: F6765) and DMSO concentration was reduced to 1%. No individual BA was detected in charcoal-stripped serum. The cultures were first incubated for 24 h in this medium in presence of BA mixtures alone to favor elimination of bovine BAs that were previously accumulated into the cells and because cholestatic drugs can alter BA uptake; then they were co-exposed to BA mixtures and the tested compounds for additional 24 h. BA mixtures were composed of 9 individual BAs at either concentrations found in the serum of normal individuals (1X) or 60-fold higher concentrations (60X). These BAs included CA, CDCA and their taurine and glycine conjugates; DCA and its glycine conjugate and LCA (Table 1). The choice of 24h-drug treatment was based on previous results (Sharanek, et al., 2017). Of note, if total BA content in the serum of patients suffering from chronic cholestatic diseases can reach 60-fold or more that measured in the serum of healthy individuals the relative changes in individual BAs are quite variable. Primary BA content is usually hugely increased while that of secondary BAs is frequently decreased (Humbert, et al., 2012; Masubuchi *et al.*, 2016; Tribe, et al., 2010; Trottier, et al., 2012). However, a significant increase in total serum LCA and DCA has been reported in pregnant women with intrahepatic cholestasis (Lucangioli *et al.*, 2009) and levels of conjugated LCA were found 30-40-fold higher in serum of heart transplant patients with chronic hepatitis compared to transplant patients without hepatitis and non-transplant patients with chronic hepatitis after treatment with CsA (Myara *et al.*, 1996). Moreover, the amounts of total LCA, DCA and CDCA in the 60X-BA mixture, i.e. 1.8, 51.6 and 135.6 μM respectively, remained much lower than their corresponding *in vitro* cytotoxic concentrations (Sharanek *et al.*, 2015; Woolbright, et al., 2015).

Cell viability

Cytotoxicity was evaluated using the MTT colorimetric assay. Briefly, the cells were seeded in 96-well plates and treated with the tested compounds in presence of the 60X-BA mixture for 24 h. After medium removal, 100 μl of serum-free medium containing MTT (0.5 mg/ml) was added to each well and incubated for 2 h at 37°C. The water-insoluble formazan was

dissolved in 100 μ l DMSO, and absorbance was measured at 550 nm.

Sample preparation and measurement of bile acids

Standard BA stock solutions were prepared in methanol at a concentration of $1\text{mg}\cdot\text{mL}^{-1}$ and stored in a sealed container at -20°C . The stock solutions were pooled and diluted to obtain mixed-calibration BA solutions with concentrations ranging from $31.3\text{ ng}\cdot\text{mL}^{-1}$ to $31.3\text{ }\mu\text{g}\cdot\text{mL}^{-1}$. Standard solutions were available for 28 BAs (Supplementary Table 1).

Both cells (by gentle scrapping) and culture media (supernatants) were collected from HepaRG cell cultures treated with the 13 tested compounds plus TRO used as a positive control, in the presence of either 1X- or 60X-BA mixture. Before analysis, the samples were lyophilized, and then 1 ml of water was added to the dried samples, homogenized using a PolyTron® homogenizer for 30 sec and clarified by centrifugation at $20,000 \times g$ for 20 min. The supernatants were collected and extracted using a SPE cartridge. BA content was measured using high pressure liquid chromatography coupled with tandem mass spectrometry (HPLC–MS/MS). The chromatographic separation of BAs was carried out on a Zorbax eclipse XDB-C18 (Agilent Technology, Garches, France) fitted on an Agilent 1100 HPLC system (Massy, France) as previously described for human samples (Humbert, et al., 2012). The column temperature setting was 35°C . The mobile phases consisted of (A) ammonium acetate 15 mmol/l, pH 5.3 and (B) methanol at 65:35 (v/v). BAs were eluted by increasing B in A from 65 to 95 (v/v) for 30 min. Separation was achieved at a flow rate varying between 0.3 and 0.5 ml/min for 30 min. Mass spectra were obtained using an API® 2000 Q-Trap (AB-Sciex, Concord, Canada) equipped with a Turbolon electrospray (ESI) interface set in the negative mode (needle voltage – 4500V) with nitrogen as the nebulizer set at 40 (arbitrary pressure unit given by the equipment provider). Curtain and heater pressures were set at 20 and 40 (arbitrary units), respectively and the ion source temperature was set at 400°C . Declustering and entrance potentials were set at -60V and -10V , respectively. The MS/MS detection was operated at unit/unit resolution. The acquisition dwell time for each transition monitored was 70 msec. Data were acquired by the

Analyst® software (version 1.4.2, AB-Sciex) in the Multiple Reaction Monitoring (MRM) mode. Depending on culture conditions, 12 BAs were detected, i.e. CDCA, GCDCA, TCDCA; CA, GCA, TCA, DCA, GDCA, TDCA, LCA, 3S-LCA and 3S-TLCA.

Data analysis

The amounts of total and individual BAs were measured in both cell layers and supernatants. HepaRG hepatocytes represent around 50% of total cells in differentiated cultures (Cerec, et al., 2007). Since primitive biliary cells do not express BA metabolizing enzymes and transporters and do not accumulate BAs (Sharanek *et al.*, 2014; Sharanek, et al., 2015), they were neglected for calculation of BA content. Each 10 cm dish was estimated to contain around 7×10^6 cells of which 3.5×10^6 HepaRG hepatocytes. To keep the same unit BA values were expressed as $\mu\text{g}/10^6$ hepatocytes in both cell layers and supernatants.

Statistical analysis

One-way ANOVA with Bonferroni's multiple comparison test (GraphPad Prism 5.00) was performed to compare data. Each value corresponded to the mean \pm standard deviation (S.D) of three independent experiments. Data were considered significantly different when $p < 0.05$.

Results

Metabolism of exogenous bile acids by HepaRG hepatocytes

Differentiated HepaRG cells were first incubated for 24 h in a medium containing 2% BA-free serum and 1% DMSO and supplemented with the mixture of 9 major BAs either at concentrations found in serum of normal individuals (1X) or at 60-fold higher concentrations (60X), and then concomitantly with the tested drugs in the same medium for additional 24 h. As previously observed (Sharanek, et al., 2017), in our experimental conditions 1X- and 60X-BA mixtures did not induce obvious cellular injury. No significant cytotoxicity was observed

using the MTT assay and only slight dilatation of BCs and/or some lipid droplets were seen in hepatocyte-like cells, if any (Figure 1).

Total 1X- and 60X-BA contents measured in unexposed media corresponded to 3.56 μM (or 4.48 $\mu\text{g}/10^6$ HepaRG hepatocytes) and 178.63 μM (or 224.89 $\mu\text{g}/10^6$ HepaRG hepatocytes), respectively. After the second 24 h incubation of HepaRG cell cultures with 1X- and 60X-BA mixtures 4.88 \pm 0.58 and 264.9 \pm 31.9 μg per 10^6 HepaRG hepatocytes were recovered in supernatants + cell layers, respectively (Table 2). These values included cellular accumulated BAs at the time of medium renewal with BA mixtures. BA contents in cell extracts represented less than 7% in both conditions. The amount of neo-synthesized BAs during this period was limited (Sharaneek, et al., 2017).

Nearly all unconjugated CA, CDCA and DCA added to the 1X-BA mixture were conjugated, mainly to taurine while LCA was completely sulfated in control cultures after the second 24 h incubation. No amidated LCA was detected. The BA mixture did not contain TDCA. Changes in glycine conjugates were limited, if any (Table 3).

Unconjugated BAs added in the 60X-mixture were also metabolized; indeed, unconjugated CDCA, DCA and CA levels were reduced and those of conjugated BAs were increased. LCA was nearly completely sulfated of which around 50% was conjugated to taurine (Table 3).

Effects of the tested compounds on cellular accumulation of BAs in presence of exogenous BAs

Seven out of the 13 new tested compounds were previously found to impair BC dynamics, causing dilatation or constriction, and were classified as cholestatic, namely FLX, BOS, PER, FAS, LVX, ERY and MAC. The 6 others did not affect BC morphology and were classified as noncholestatic (SM, SIT, APAP, AMI, AMB and AMP), in agreement with clinical observations (Burbank, et al., 2016); they corresponded to 3 hepatotoxic (AMI, APAP, SIT) and 3 nonhepatotoxic (SM, AMB, AMP) compounds. In addition, TRO was used as a positive cholestatic drug to make direct comparison with our previously reported observations

(Sharanek, et al., 2017). Drugs were added at the following concentrations: TRO, BOS, FAS, ERY, MAC, PER, AMI: 10 μ M; FLX: 0.5mM; LVX, AMB, SIT: 50 μ M; SM, AMP, APAP: 2mM (Table 4). These concentrations were selected from preliminary dose-response cytotoxicity studies. Since the 60X-BA mixture enhanced cytotoxicity induced by hepatotoxic drugs lower concentrations than those previously selected for evaluation of their effects on BC dynamics and morphology, had to be used. In the current experimental conditions, in absence or presence of BA mixtures, dilatation of BC was observed in HepaRG hepatocytes treated with most cholestatic drugs, especially FAS and FLX. No other obvious morphological changes and no significant decrease in MTT values were evidenced after 24 h treatments (Figure 1). Comparable total BA levels (supernatants + cell layers) were recovered after incubation of the cultures with either BA mixtures whatever the culture condition (drug treatment or not) (Table 2).

Effects of noncholestatic drugs

Whether incubated in the presence of 1X- or 60X-BA mixtures, cultures treated with noncholestatic drugs exhibited comparable changes to those observed in cultures treated with drugs only. Comparable BA values (total and individual BAs) to those measured in control cultures were found in cultures treated with noncholestatic drugs for 24 h. Nearly all CA, CDCA and DCA that were present in the 1X-BA mixture, were conjugated while LCA was completely sulfated. No amidated LCA was detected. A large fraction of CA and DCA added to the 60X-BA mixture was also conjugated to taurine; CDCA was only partly conjugated and LCA was mostly sulfated, either as 3S-LCA or 3S-TLCA at nearly equal percentages. Both forms of LCA were present mostly in the supernatants and only as traces in cell layers of untreated cultures. In addition, low amounts of unconjugated/unsulfated LCA were detected in supernatants from cultures treated with APAP, AMI and AMB. Levels of cellular unconjugated BAs found with noncholestatic drugs were comparable to those measured in control cultures (Figures 2-4 and Supplementary Tables 2 and 3).

Effects of cholestatic drugs in presence of the 1X-BA mixture

Among the 7 new tested cholestatic drugs only FAS showed a significant cellular increase (2.4-fold) in total BAs, peaking at 0.69 μg , a value close to that found with TRO (Figure 2A). These major changes in total BAs observed with TRO and FAS were associated with marked increase in unconjugates/conjugates ratios of hydrophobic BAs. Indeed, in supernatants from TRO- and FAS-treated cultures levels of unconjugated CDCA were around 30-fold higher whereas those of its conjugates (TCDCA and GCDCA) were reduced when compared to the values obtained with other cholestatic drugs (Figure 2B). Marked unconjugated DCA levels were detected only in supernatants of TRO-treated cultures (0.2 μg) and in parallel, conjugates were reduced by around 35-45% (TDCA) or 20-30% (GDCA). Importantly, cellular accumulation of unconjugated CDCA and DCA was evidenced only with these two drugs, i.e. 0.05 and 0.11 μg with TRO and 0.04 and 0.03 μg with FAS respectively (Figure 2C and supplementary Table 2). Although it was not added in the mixture, TDCA was detected in both supernatants and cell layers at comparable levels in all samples, except in those from TRO-treated cultures (Supplementary Table 2).

While LCA was undetectable in cell layers from untreated cells, it reached 17.5, 7.5, 5, 6, 10, 7, 7 and 2 ng in cell layers of TRO, FLX-, BOS-, PER-, FAS-, LVX-, ERY- and MAC-treated cultures respectively, after 24 h, (Figure 2D). Total LCA was found in its sulfated form, except in TRO-treated cultures. Indeed in these latter, unsulfated LCA was detected in both supernatants and cell layers (Figure 2E); in parallel, the levels of sulfated LCA were strongly decreased (>60%, corresponding to around 0.03 μg) in supernatants (Figure 2E and F).

Much more limited changes were observed in CA levels. Unconjugated CA was increased around 3 times in supernatants of TRO- and FAS-treated cells and traces were detected in cell layers of TRO-treated cells only (Figure 2G).

Effects of cholestatic drugs in presence of the 60X-BA mixture

A 1.7 to 2.7-fold increase in total BAs was evidenced in cell layers of HepaRG cell cultures treated with cholestatic drugs, in presence of the 60X-BA mixture when compared to corresponding controls (Figure 3A). The value measured with TRO was similar to that found

with most other cholestatic drugs. In parallel, BA levels were decreased in supernatants. Accordingly, major changes were observed in cellular and supernatant profiles of hydrophobic BAs from cultures treated with cholestatic drugs. Enhanced cellular accumulation of total BAs was associated with around 4- to 8-fold more unconjugates and 2-3-fold more conjugates of CDCA and DCA as well as increased unsulfated LCA (Figure 3B). Cellular accumulation of the 3 hydrophobic BAs, CDCA, DCA and LCA, in their unconjugated or unsulfated forms was evidenced with the 8 cholestatic drugs (Figure 3C, D; Figure 4; Supplementary Table 3). LCA was the most accumulated BA. Total cellular LCA (unconjugated and sulfated forms) reached 0.23 to 0.61 μg ; i.e. 9 to 24% of total LCA. Unsulfated LCA represented 0.06 to 0.27 μg (Figure 4A and B). In corresponding supernatant levels of unsulfated LCA reached 0.5 to 1.2 μg while only traces were detected in controls and in cultures treated with noncholestatic molecules, if any (Figure 4C and D). Limited changes were observed in CA profiles in cultures treated with cholestatic compounds. Importantly, unconjugated CA was evidenced only in supernatants (Figure 4F).

Discussion

Many drugs are known to induce cholestasis in a minority of patients but little information exists on accumulation of toxic BAs in the liver. In the current study, using a large set of cholestatic and noncholestatic drugs we show that only the former caused preferential cellular accumulation of hydrophobic BAs in HepaRG hepatocytes after 24h-co-exposure with a mixture of exogenous BAs at concentrations usually found in serum of healthy subjects and/or at 60-fold higher concentrations. CDCA and DCA preferentially accumulated as unconjugates and LCA in its unsulfated form.

Intrahepatic accumulation of hydrophobic BAs is considered as the hallmark of cholestasis. CDCA, DCA, LCA and GCDCA have been reported to be highly cytotoxic in rodents, and their accumulation can damage hepatic cells by inducing mitochondrial dysfunction, oxidative stress or apoptosis (Malhi *et al.*, 2010). However, hydrophobic BAs are much less hepatotoxic in human than in various animal species (Hofmann, 2004; Woolbright, *et al.*,

2015). In agreement, after 24-hour exposure, GCDCA was found to cause necrosis of primary human hepatocytes (Woolbright, et al., 2015) and LCA to be cytotoxic to HepaRG cells (Sharaneek, et al., 2015), only at concentrations of 1 mM and 100 μ M, respectively. Overall concentrations of serum and bile BA concentrations usually observed during cholestasis *in vivo* ranged from 1 to 20 μ M and 1 to 5 mM respectively (Woolbright, et al., 2015); consequently, serum levels must be supplemented with hydrophobic BAs to become hepatotoxic to isolated hepatocytes and liver cell lines.

Addition of BAs to the medium is a prerequisite to detect accumulation in *in vitro* hepatocytes. Indeed, in BA-free medium the amounts of neo-synthesized BAs are limited and strongly reduced by cholestatic drugs (Sharaneek, et al., 2015). Total cellular BAs could reach 50 μ g/ 10^6 hepatocytes after 24h-treatment with cholestatic drugs compared to 17 μ g/ 10^6 hepatocytes in corresponding untreated cultures, in presence of the 60X-BA mixture, without evidence of cellular injury. Comparable cellular accumulation of BAs was obtained with CsA, CPZ and TRO (Sharaneek, et al., 2017). Altogether, these data favor the conclusion that in our *in vitro* experimental conditions cholestatic drugs can cause features of cholestasis in absence of marked cellular damage and agree with the prolonged survival of hepatocytes in cholestatic livers despite high intrahepatic and serum BA levels. However, importantly when higher noncytotoxic cholestatic drug concentrations were used morphological alterations that included accumulation of intracytoplasmic lipid droplets and detachment of primitive biliary cells, occurred in presence of the 60X-BA mixture after 24h co-treatment, reflecting mixed hepatocellular-cholestatic lesions (not shown). Recent studies have shown that BAs might induce liver cell injury either *in vitro* or *in vivo* in an inflammatory context (Cai *et al.*, 2017; Hao *et al.*, 2017; Woolbright *et al.*, 2016). It might be hypothesized that in presence of pro-inflammatory cytokines or innate immune cells HepaRG cells will be more sensitive to cellular accumulation of BAs caused by cholestatic drugs. This important question warrants further investigation.

HepaRG cells actively conjugated BAs as shown by disappearance of unconjugated CDCA, DCA and CA and appearance of large amounts of corresponding conjugates in presence of

BA mixtures after 24h-incubation. Preferential formation of taurine conjugates from the 3 BAs agrees with previous observations (Sharanek, et al., 2017).

Major differences were observed in supernatant/cell extract ratios and profiles of BAs in cultures treated with cholestatic drugs compared to cultures that were either untreated or treated with noncholestatic compounds, especially in presence of 60X-BA mixture. When using a medium containing the major BAs at concentrations found in the serum of healthy subjects peculiar changes in BA profiles were evidenced with two out of the tested cholestatic drugs, i.e. TRO and FAS; that were mainly characterized by lower conjugation of CDCA and CDA associated with reduced accumulation of taurine and glycine conjugates in the supernatants. However, the most important changes observed in presence of 1X-BA mixture concerned LCA, the most lipophilic BA, that was detected in cell layers from cultures treated with all cholestatic drugs. Noteworthy, cellular LCA was previously evidenced in cultures treated with CPZ, CsA and TRO after 4 h in presence of 1X-BA mixture (Sharanek, et al., 2017); it was also detected in HepaRG cells after 4h and 24h treatment with 10 or 50 μM CsA in presence of 2% bovine serum, containing $16.8 \pm 3.3 \text{ nM}$ LCA, i.e. around $1.8 \text{ ng}/10^6$ hepatocytes (Sharanek, et al., 2015). Altogether, these results suggest that LCA is the first hydrophobic BA to accumulate in hepatocytes treated with cholestatic drugs.

More extensive changes were found with all tested cholestatic drugs after 24h-co-incubation with the 60X-BA mixture. They were typified by more unconjugated BAs (CDCA, CA and DCA), lower amounts of their taurine and glycine conjugates and presence of unsulfated LCA in supernatants and in parallel, preferential accumulation of unconjugated CDCA and DCA and unsulfated LCA in cell layers, favoring the conclusion that inhibition of BA amidation and sulfation activities could be a common effect of cholestatic drugs. In support, gene expression of the conjugating CoA:amino acid N-acyltransferase (BAAT) was found to be inhibited by 36% and 84% after 4 h and 24 h treatment with 50 μM CsA in a medium containing 2% bovine serum and 1% DMSO, respectively (Sharanek, et al., 2015). Further studies are warranted to determine the precise mechanisms by which conjugation and sulfation of BAs are inhibited by cholestatic drugs.

In addition to unconjugated LCA, cellular accumulation of 3S-TLCA and 3S-LCA was evidenced after treatment with all cholestatic drugs at variable levels in presence of the 60X-BA mixture. Noticeably, cellular LCA content (unconjugated LCA, 3S-TLCA and 3S-LCA) represented >21% with TRO, BOS and FLX, 3 potent cholestatic drugs, versus 15% or less with other cholestatic drugs, of total recovered LCA (cell layers + supernatants). These data suggest that in addition to inhibition of LCA sulfation cholestatic drugs reduced excretion of the sulfated forms. Intracellular accumulation of 3S-TLCA could result from inhibition of its efflux transport.

Although also specifically observed with cholestatic drugs the increase in cellular unconjugated CA was lower compared to unconjugated hydrophobic BAs. Contrary to the latter that freely diffuse across membranes, CA requires a carrier for hepatocyte uptake (Hofmann, 2004); this could lead to a lower uptake and consequently lower accumulation in HepaRG hepatocytes.

The cholestatic drugs included the recently marketed endothelin receptor antagonist MAC. Despite no known or suspected cases of cholestasis in patients suffering from pulmonary arterial hypertension it was demonstrated to exhibit similar hepatotoxic and cholestatic properties to bosentan, using HepaRG hepatocytes. Its similar chemical structure to bosentan, was advanced to sustain its *in vitro* cholestatic properties (Burbank *et al.*, 2017). Its ability to cause cellular accumulation of unconjugated BAs supports its classification as a cholestatic drug. Noteworthy, a first case of acute liver failure with a process of micronodular cholestatic cirrhosis was recently associated with MAC treatment (Tran *et al.*, 2018).

Many cholestatic drugs have been identified as inhibitors of the bile salt export pump (BSEP) using inverted membrane vesicles (Dawson *et al.*, 2012; Morgan *et al.*, 2010; Pedersen *et al.*, 2013). However, false positives and false negatives have been found (Pedersen, *et al.*, 2013). For instance, the potent cholestatic CPZ was classified as a non BSEP inhibitor and the noncholestatic AMI as a weak BSEP inhibitor (Morgan, *et al.*, 2010). Interestingly, our results demonstrate that measurement of toxic hydrophobic BAs allowed to correctly classify CPZ and AMI as cholestatic and noncholestatic respectively. Recently, Chan and Benet

examined several published BSEP inhibition datasets and concluded that this assay is not predictive of cholestatic potential of drugs (Chan *et al.*, 2018). Another assay, the drug induced cholestasis index, based on inhibition of urea production in sandwich-cultured human hepatocytes co-exposed to drugs and a BA mixture, has been proposed to identify drugs with cholestatic risk (Oorts *et al.*, 2016). This index likely reflects BA-enhanced sensitivity to hepatotoxic compounds; compared to our own approach it usually requires higher drug concentrations and does not identify all cholestatic drugs.

Recently, adverse outcome pathways (AOPs) have been introduced as new tools to gain knowledge on the mechanism basis of toxicity. They include molecular initiating events and a series of key intermediate events, leading to a toxic effect. The first AOP for cholestasis was based on the inhibition of BSEP (Vinken *et al.*, 2013). Since this assay does not reflect a general mechanism of cholestatic drugs mechanistic modelling of cholestasis in AOP networks are now considered as more appropriate. Our previous and present studies have identified new key events that have been observed with all the hitherto tested potent cholestatic drugs; i.e. deregulation of the ROCK-MLCK pathway, impairment of BC dynamics associated with disruption of pericanalicular actin filaments, that, in addition to inhibition of transporters, can result in preferential cellular accumulation of toxic hydrophobic BAs. All these key events could be used to define new AOPs for cholestasis.

In summary, our results show that cholestatic drugs can specifically cause rapid and preferential accumulation of toxic hydrophobic BAs, especially LCA, in HepaRG hepatocytes and that the huge increase in unconjugated versus conjugated forms, appears to reflect what is occurring in cholestatic livers (Abukawa, *et al.*, 1998; Fischer, *et al.*, 1996). Together with BC dynamics impairment cellular accumulation of these BAs could represent potent biomarkers of the cholestatic potential of new compounds and could be used to test therapeutics for cholestatic liver injury. Cellular BA accumulation could be measured not only by HPLC-MS/MS but also by the use of fluorescent BA probes. These results give further support to the suitability of

differentiated HepaRG cells for investigations on mechanisms of drug-induced cholestasis as well as for other toxicity studies (Guillouzo *et al.*, 2018).

Acknowledgments

We are grateful to Coralie Allain for her help with some HepaRG cell cultures. This work was partly supported by the European Community through the Innovative Medicines Initiative Joint Undertaking MIP-DILI project [grant agreement number 115336], resources of which are composed of financial contribution from the European Union's Seventh Framework Programme [FP7/20072013] and EFPIA companies' in kind contribution. Audrey Burban and Ahmad Sharaneq were financially supported by the MIP-DILI project.

References

- Abukawa, D., Nakagawa, M., Inuma, K., Nio, M., Ohi, R., and Goto, J. (1998). Hepatic and serum bile acid compositions in patients with biliary atresia: a microanalysis using gas chromatography-mass spectrometry with negative ion chemical ionization detection. *The Tohoku journal of experimental medicine* **185**(4), 227-37.
- Akaho, E., Maekawa, T., Uchinashi, M., and Kanamori, R. (2002). A study of streptomycin blood level information of patients undergoing hemodialysis. *Biopharmaceutics & drug disposition* **23**(2), 47-52.
- Antherieu, S., Bachour-El Azzi, P., Dumont, J., Abdel-Razzak, Z., Guguen-Guillouzo, C., Fromenty, B., Robin, M. A., and Guillouzo, A. (2013). Oxidative stress plays a major role in chlorpromazine-induced cholestasis in human HepaRG cells. *Hepatology* **57**(4), 1518-29.
- Anwer, M. S. (2014). Role of protein kinase C isoforms in bile formation and cholestasis. *Hepatology* **60**(3), 1090-7.
- Burban, A., Sharanek, A., Guguen-Guillouzo, C., and Guillouzo, A. (2018). Endoplasmic reticulum stress precedes oxidative stress in antibiotic-induced cholestasis and cytotoxicity in human hepatocytes. *Free radical biology & medicine* **115**, 166-178.
- Burban, A., Sharanek, A., Hue, R., Gay, M., Routier, S., Guillouzo, A., and Guguen-Guillouzo, C. (2017). Penicillinase-resistant antibiotics induce non-immune-mediated cholestasis through HSP27 activation associated with PKC/P38 and PI3K/AKT signaling pathways. *Scientific reports* **7**(1), 1815.
- Burbank, M. G., Burban, A., Sharanek, A., Weaver, R. J., Guguen-Guillouzo, C., and Guillouzo, A. (2016). Early Alterations of Bile Canaliculi Dynamics and the Rho Kinase/Myosin Light Chain Kinase Pathway Are Characteristics of Drug-Induced Intrahepatic Cholestasis. *Drug metabolism and disposition: the biological fate of chemicals* **44**(11), 1780-1793.
- Burbank, M. G., Sharanek, A., Burban, A., Mialanne, H., Aerts, H., Guguen-Guillouzo, C., Weaver, R. J., and Guillouzo, A. (2017). From the Cover: Mechanistic Insights in Cytotoxic and Cholestatic Potential of the Endothelial Receptor Antagonists Using HepaRG Cells. *Toxicological sciences : an official journal of the Society of Toxicology* **157**(2), 451-464.
- Cai, S. Y., Ouyang, X., Chen, Y., Soroka, C. J., Wang, J., Mennone, A., Wang, Y., Mehal, W. Z., Jain, D., and Boyer, J. L. (2017). Bile acids initiate cholestatic liver injury by triggering a hepatocyte-specific inflammatory response. *JCI insight* **2**(5), e90780.
- Castano, G., Lucangioli, S., Sookoian, S., Mesquida, M., Lemberg, A., Di Scala, M., Franchi, P., Carducci, C., and Tripodi, V. (2006). Bile acid profiles by capillary electrophoresis in intrahepatic cholestasis of pregnancy. *Clinical science* **110**(4), 459-65.
- Cerec, V., Glaise, D., Garnier, D., Morosan, S., Turlin, B., Drenou, B., Gripon, P., Kremsdorf, D., Guguen-Guillouzo, C., and Corlu, A. (2007). Transdifferentiation of hepatocyte-like cells from the human hepatoma HepaRG cell line through bipotent progenitor. *Hepatology* **45**(4), 957-67.
- Chan, R., and Benet, L. Z. (2018). Measures of BSEP Inhibition In Vitro Are Not Useful Predictors of DILI. *Toxicological sciences : an official journal of the Society of Toxicology* **162**(2), 499-508.
- Chiang, J. Y. (2009). Bile acids: regulation of synthesis. *Journal of lipid research* **50**(10), 1955-66.
- Dawson, S., Stahl, S., Paul, N., Barber, J., and Kenna, J. G. (2012). In vitro inhibition of the bile salt export pump correlates with risk of cholestatic drug-induced liver injury in humans. *Drug metabolism and disposition: the biological fate of chemicals* **40**(1), 130-8.

- Fattinger, K., Funk, C., Pantze, M., Weber, C., Reichen, J., Stieger, B., and Meier, P. J. (2001). The endothelin antagonist bosentan inhibits the canalicular bile salt export pump: a potential mechanism for hepatic adverse reactions. *Clinical pharmacology and therapeutics* **69**(4), 223-31.
- Fischer, S., Beuers, U., Spengler, U., Zwiebel, F. M., and Koebe, H. G. (1996). Hepatic levels of bile acids in end-stage chronic cholestatic liver disease. *Clinica chimica acta; international journal of clinical chemistry* **251**(2), 173-86.
- Fish, D. N., and Chow, A. T. (1997). The clinical pharmacokinetics of levofloxacin. *Clinical pharmacokinetics* **32**(2), 101-19.
- Fukumoto, Y., Matoba, T., Ito, A., Tanaka, H., Kishi, T., Hayashidani, S., Abe, K., Takeshita, A., and Shimokawa, H. (2005). Acute vasodilator effects of a Rho-kinase inhibitor, fasudil, in patients with severe pulmonary hypertension. *Heart* **91**(3), 391-2.
- Garcia-Canaveras, J. C., Donato, M. T., Castell, J. V., and Lahoz, A. (2012). Targeted profiling of circulating and hepatic bile acids in human, mouse, and rat using a UPLC-MRM-MS-validated method. *Journal of lipid research* **53**(10), 2231-41.
- Gardiner, S. J., Drennan, P. G., Begg, R., Zhang, M., Green, J. K., Isenman, H. L., Everts, R. J., Chambers, S. T., and Begg, E. J. (2018). In healthy volunteers, taking flucloxacillin with food does not compromise effective plasma concentrations in most circumstances. *PloS one* **13**(7), e0199370.
- Geerdes-Fenge, H. F., Goetschi, B., Rau, M., Borner, K., Koeppe, P., Wettich, K., and Lode, H. (1997). Comparative pharmacokinetics of dirithromycin and erythromycin in normal volunteers with special regard to accumulation in polymorphonuclear leukocytes and in saliva. *European journal of clinical pharmacology* **53**(2), 127-33.
- Guillouzo, A., and Guguen-Guillouzo, C. (2018). HepaRG Cells as a Model for Hepatotoxicity Studies. In *In Stem cells in toxicology and teratology* (T. P. R. (Ed.), Ed.) doi: doi:10.1002/9781119283249.ch12, pp. 309-339. Hoboken, NJ, USA John Wiley & Sons, Inc.
- Hao, H., Cao, L., Jiang, C., Che, Y., Zhang, S., Takahashi, S., Wang, G., and Gonzalez, F. J. (2017). Farnesoid X Receptor Regulation of the NLRP3 Inflammasome Underlies Cholestasis-Associated Sepsis. *Cell metabolism* **25**(4), 856-867 e5.
- Hofmann, A. F. (2004). Detoxification of lithocholic acid, a toxic bile acid: relevance to drug hepatotoxicity. *Drug metabolism reviews* **36**(3-4), 703-22.
- Humbert, L., Maubert, M. A., Wolf, C., Duboc, H., Mahe, M., Farabos, D., Seksik, P., Mallet, J. M., Trugnan, G., Masliah, J., et al. (2012). Bile acid profiling in human biological samples: comparison of extraction procedures and application to normal and cholestatic patients. *J Chromatogr B Analyt Technol Biomed Life Sci* **899**, 135-45.
- Layden, T. J., Schwarz, and Boyer, J. L. (1975). Scanning electron microscopy of the rat liver. Studies of the effect of taurolithocholate and other models of cholestasis. *Gastroenterology* **69**(3), 724-38.
- Lucangioli, S. E., Castano, G., Contin, M. D., and Tripodi, V. P. (2009). Lithocholic acid as a biomarker of intrahepatic cholestasis of pregnancy during ursodeoxycholic acid treatment. *Ann Clin Biochem* **46**(Pt 1), 44-9.
- Malhi, H., Guicciardi, M. E., and Gores, G. J. (2010). Hepatocyte death: a clear and present danger. *Physiological reviews* **90**(3), 1165-94.
- Masubuchi, N., Sugihara, M., Sugita, T., Amano, K., Nakano, M., and Matsuura, T. (2016). Oxidative stress markers, secondary bile acids and sulfated bile acids classify the clinical liver injury type: Promising diagnostic biomarkers for cholestasis. *Chemico-biological interactions* **255**, 83-91.

- Monte, M. J., Marin, J. J., Antelo, A., and Vazquez-Tato, J. (2009). Bile acids: chemistry, physiology, and pathophysiology. *World journal of gastroenterology* **15**(7), 804-16.
- Morgan, R. E., Trauner, M., van Staden, C. J., Lee, P. H., Ramachandran, B., Eschenberg, M., Afshari, C. A., Qualls, C. W., Jr., Lightfoot-Dunn, R., and Hamadeh, H. K. (2010). Interference with bile salt export pump function is a susceptibility factor for human liver injury in drug development. *Toxicological sciences : an official journal of the Society of Toxicology* **118**(2), 485-500.
- Myara, A., Cadranet, J. F., Dorent, R., Lunel, F., Bouvier, E., Gerhardt, M., Bernard, B., Ghossoub, J. J., Cabrol, A., Gandjbakhch, I., et al. (1996). Cyclosporin A-mediated cholestasis in patients with chronic hepatitis after heart transplantation. *Eur J Gastroenterol Hepatol* **8**(3), 267-71.
- Oorts, M., Baze, A., Bachellier, P., Heyd, B., Zacharias, T., Annaert, P., and Richert, L. (2016). Drug-induced cholestasis risk assessment in sandwich-cultured human hepatocytes. *Toxicology in vitro : an international journal published in association with BIBRA* **34**, 179-86.
- Pedersen, J. M., Matsson, P., Bergstrom, C. A., Hoogstraate, J., Noren, A., LeCluyse, E. L., and Artursson, P. (2013). Early identification of clinically relevant drug interactions with the human bile salt export pump (BSEP/ABCB11). *Toxicological sciences : an official journal of the Society of Toxicology* **136**(2), 328-43.
- Reyes, H., and Sjoval, J. (2000). Bile acids and progesterone metabolites in intrahepatic cholestasis of pregnancy. *Annals of medicine* **32**(2), 94-106.
- Scherer, M., Gnewuch, C., Schmitz, G., and Liebisch, G. (2009). Rapid quantification of bile acids and their conjugates in serum by liquid chromatography-tandem mass spectrometry. *J Chromatogr B Analyt Technol Biomed Life Sci* **877**(30), 3920-5.
- Sharanek, A., Azzi, P. B., Al-Attrache, H., Savary, C. C., Humbert, L., Rainteau, D., Guguen-Guillouzo, C., and Guillouzo, A. (2014). Different dose-dependent mechanisms are involved in early cyclosporine a-induced cholestatic effects in hepaRG cells. *Toxicological sciences : an official journal of the Society of Toxicology* **141**(1), 244-53.
- Sharanek, A., Burban, A., Burbank, M., Le Guevel, R., Li, R., Guillouzo, A., and Guguen-Guillouzo, C. (2016). Rho-kinase/myosin light chain kinase pathway plays a key role in the impairment of bile canaliculi dynamics induced by cholestatic drugs. *Scientific reports* **6**, 24709.
- Sharanek, A., Burban, A., Humbert, L., Bachour-EI Azzi, P., Felix-Gomes, N., Rainteau, D., and Guillouzo, A. (2015). Cellular Accumulation and Toxic Effects of Bile Acids in Cyclosporine A-Treated HepaRG Hepatocytes. *Toxicological sciences : an official journal of the Society of Toxicology* **147**(2), 573-87.
- Sharanek, A., Burban, A., Humbert, L., Guguen-Guillouzo, C., Rainteau, D., and Guillouzo, A. (2017). Progressive and Preferential Cellular Accumulation of Hydrophobic Bile Acids Induced by Cholestatic Drugs Is Associated with Inhibition of Their Amidation and Sulfation. *Drug metabolism and disposition: the biological fate of chemicals* **45**(12), 1292-1303.
- Tran, T. T., Brinker, A. D., and Munoz, M. (2018). Serious Liver Injury Associated with Macitentan: A Case Report. *Pharmacotherapy* **38**(2), e22-e24.
- Tribe, R. M., Dann, A. T., Kenyon, A. P., Seed, P., Shennan, A. H., and Mallet, A. (2010). Longitudinal profiles of 15 serum bile acids in patients with intrahepatic cholestasis of pregnancy. *The American journal of gastroenterology* **105**(3), 585-95.
- Trottier, J., Bialek, A., Caron, P., Straka, R. J., Heathcote, J., Milkiewicz, P., and Barbier, O. (2012). Metabolomic profiling of 17 bile acids in serum from patients with primary biliary cirrhosis and primary sclerosing cholangitis: a pilot study. *Digestive and liver disease : official journal of the Italian Society of Gastroenterology and the Italian Association for the Study of the Liver* **44**(4), 303-10.

Vinken, M., Landesmann, B., Goumenou, M., Vinken, S., Shah, I., Jaeschke, H., Willett, C., Whelan, M., and Rogiers, V. (2013). Development of an adverse outcome pathway from drug-mediated bile salt export pump inhibition to cholestatic liver injury. *Toxicological sciences : an official journal of the Society of Toxicology* **136**(1), 97-106.

Wise, R., Andrews, J. M., Matthews, R., and Wolstenholme, M. (1992). The in-vitro activity of two new quinolones: rifloxacin and MF 961. *The Journal of antimicrobial chemotherapy* **29**(6), 649-60.

Woolbright, B. L., Dorko, K., Antoine, D. J., Clarke, J. I., Gholami, P., Li, F., Kumer, S. C., Schmitt, T. M., Forster, J., Fan, F., *et al.* (2015). Bile acid-induced necrosis in primary human hepatocytes and in patients with obstructive cholestasis. *Toxicology and applied pharmacology* **283**(3), 168-77.

Woolbright, B. L., and Jaeschke, H. (2016). Therapeutic targets for cholestatic liver injury. *Expert opinion on therapeutic targets* **20**(4), 463-75.

Figure legends

Figure 1. Cytotoxicity and morphological effects of the 60X-BA mixture and tested drugs in human HepaRG cell cultures.

(A) Cytotoxicity of the 60X-BA mixture and tested drugs using the MTT colorimetric assay. HepaRG cells were treated with the 60X-BA mixture alone for 24 h and then with tested drugs combined with BA mixture for additional 24h. Data were expressed relative to those of untreated cells arbitrarily set at 100%. They represent the means \pm S.D of three independent experiments. No significant change was observed. (B) Representative phase-contrast images of HepaRG cells treated with tested drugs alone or in combination with the 60X-BA mixture for 24 h. Images were captured using phase-contrast microscopy (bar = 50 μ m). Orange arrows indicate BC dilatation. No evidence of BC dilatation was observed in cultures treated with PER, APA and AMI.

Figure 2. Effects of 24-h treatment with tested drugs on BA profiles in HepaRG cell cultures incubated with the 1X-BA mixture

(A) Total BAs; (B) Unconjugated CDCA; (C) Unconjugated DCA; (D) Total LCA; (E) 3S-LCA; (F) Unsulfated LCA and (G) Unconjugated CA in supernatants and cell layers. Both total and individual BAs were calculated in μ g/10⁶ hepatocytes/24 hours. Values represent the mean \pm S.D of three independent experiments. *P < 0.05 compared with the values in cell layers of untreated cells; #P < 0.05 compared with the values in supernatants of untreated cells; and \$P < 0.05 compared with the values in cells + supernatants of untreated cells.

Figure 3. Effects of 24-h treatment with tested drugs on BA profiles in HepaRG cell cultures incubated with the 60X-BA mixture

(A) Total BAs; (B) Cellular accumulation of conjugated and unconjugated BAs; (C) Unconjugated DCA and (D) Unconjugated CDCA, in supernatants and cell layers. Both total and individual BAs were calculated in μ g/10⁶ hepatocytes/24 hours. Values represent the mean \pm S.D of three independent experiments. *P < 0.05 compared with the values in cell layers of untreated cells; #P < 0.05 compared with the values in supernatants of untreated cells; and \$P < 0.05 compared with the values in cells + supernatants of untreated cells.

Figure 4. Effects of 24-hour treatment with tested drugs on LCA profiles in HepaRG cell cultures incubated with the 60X-BA mixture

(A) Total LCA; (B) Unconjugated LCA; (C) 3S-LCA and (D) 3S-TLCA in cell layers and supernatants. LCA was calculated in μ g/10⁶ hepatocytes/24 hours. Values represent the mean \pm S.D of three independent experiments. *P < 0.05 compared with the values in cell layers of untreated cells; #P < 0.05 compared with the values in supernatants of untreated cells; and \$P < 0.05 compared with the values in cells + supernatants of untreated cells.

Table 1:

Concentrations of selected individual BAs in 1X- and 60X-BA mixtures and corresponding quantities recovered after addition to un-exposed media

	BA mixtures (μM)		Individual BAs recovered after addition to un-exposed media			
	1X	60X	1X-mixture		60X-mixture	
			μM	$\mu\text{g}/10^6$ hepatocytes	μM	$\mu\text{g}/10^6$ hepatocytes)
CDCA	0.34	20.4	0.37 \pm 0.04	0.42 \pm 0.04	19.81 \pm 0.93	22.21 \pm 1.04
TCDC	0.21	12.6	0.20 \pm 0.01	0.30 \pm 0.02	10.71 \pm 0.67	15.29 \pm 0.95
GCDCA	1.71	102.6	1.64 \pm 0.28	2.11 \pm 0.36	82.43 \pm 1.42	105.86 \pm 1.82
CA	0.20	12.0	0.18 \pm 0.02	0.21 \pm 0.02	8.83 \pm 1.29	10.31 \pm 1.51
TCA	0.048	2.88	0.06 \pm 0.01	0.08 \pm 0.01	2.24 \pm 0.02	3.30 \pm 0.03
GCA	0.41	24.6	0.30 \pm 0.01	0.40 \pm 0.02	18.65 \pm 0.92	24.81 \pm 1.23
LCA	0.03	1.8	0.04 \pm 0.01	0.05 \pm 0.01	1.63 \pm 0.11	2.25 \pm 0.15
DCA	0.48	28.8	0.40 \pm 0.02	0.45 \pm 0.02	19.75 \pm 0.61	22.14 \pm 0.69
GDCA	0.38	22.8	0.36 \pm 0.03	0.46 \pm 0.04	14.58 \pm 1.33	18.72 \pm 1.71

1X and 60X mixtures of individual BAs and quantities recovered after addition to unexposed culture media. 1X-BAs represent physiological (normal) serum concentrations (Scherer *et al.*, 2009) and 60X-BAs correspond to 60-fold higher concentrations of each BA. Corresponding quantity of each individual BA available for 10^6 hepatocytes was calculated using the following formula: Quantity ($\mu\text{g}/10^6$ hepatocytes) = Concentration* molecular weight* volume of medium / number of hepatocytes. Based on medium volume = 10ml and number of hepatocytes = 3.5×10^6 hepatocytes per dish.

Table 2: Quantity of total BAs measured in cell layers and supernatants of cultures supplemented with 1X- or 60X-BA mixtures after 24 hours

	1X-BA mixture			60X-BA mixture		
	Cells	Supernatant	Total	Cells	Supernatant	Total
Control	0.29 ± 0.05	4.59 ± 0.53	4.88	17.1 ± 2.2	247.8 ± 29.7	264.9
Streptomycin	0.29 ± 0.10	4.28 ± 0.50	4.57	15.7 ± 3.1	251.5 ± 26.4	267.2
Sitaxentan	0.12 ± 0.05	4.78 ± 0.72	4.90	19.3 ± 3.3	250.7 ± 21.4	270.0
Acetaminophen	0.18 ± 0.06	4.55 ± 0.61	4.73	13.0 ± 2.5	245.3 ± 27.8	258.3
Amiodarone	0.16 ± 0.05	4.80 ± 0.59	4.96	15.9 ± 3.2	245.2 ± 26.6	261.1
Ambrisentan	0.21 ± 0.03	4.82 ± 0.70	5.03	11.7 ± 2.1	249.2 ± 31.7	260.9
Ampicillin	0.12 ± 0.04	4.81 ± 0.51	4.93	16.6 ± 2.7	251.6 ± 30.0	268.2
Troglitazone	0.63 ± 0.08	4.50 ± 0.60	5.13	43.3 ± 6.8	220.8 ± 23.0	263.3
Flucloxacillin	0.22 ± 0.07	4.58 ± 0.45	4.80	42.7 ± 7.5	215.5 ± 23.8	258.2
Bosentan	0.22 ± 0.08	5.22 ± 0.65	5.44	46.7 ± 8.7	215.5 ± 23.5	262.2
Perhexilline	0.31 ± 0.07	4.68 ± 0.53	4.99	33.7 ± 6.9	224.5 ± 25.6	258.2
Fasudil	0.69 ± 0.16	4.61 ± 0.63	5.30	29.3 ± 5.0	229.2 ± 26.9	258.5
Levofloxacin	0.38 ± 0.14	4.10 ± 0.40	4.48	39.2 ± 7.1	223.2 ± 25.9	262.4
Erythromycin	0.19 ± 0.04	4.56 ± 0.37	4.75	39.8 ± 10	220.3 ± 28.6	260.1
Macitentan	0.17 ± 0.04	4.56 ± 0.67	4.73	32.1 ± 7.6	228.1 ± 30.4	260.2

Values are expressed as $\mu\text{g}/10^6$ hepatocytes.

Table 3: Changes in bile acid profiles after incubation of untreated HepaRG hepatocytes with BA mixtures for 24h.

	1X-BA mixture		60X-BA mixture	
	Unexposed medium	Untreated cultures	Unexposed medium	Untreated cultures
CDCA	0.42± 0.04	0.01±0.0	22.21 ± 1.04	19.78±4.3
GCDCA	2.11 ± 0.36	2.22±0.24	105.86 ± 1.82	128.0±8.5
TCDC	0.30 ± 0.02	0.94±0.12	15.29 ± 0.95	35.20±3.3
CA	0.21 ± 0.02	0.05±0.01	10.31 ± 1.51	7.80±0.8
GCA	0.40 ± 0.02	0.42±0.02	24.81 ± 1.23	22.70±0.6
TCA	0.08 ± 0.01	0.31±0.03	3.30 ± 0.03	5.0±0.1
LCA	0.05 ± 0.01	0	2.25 ± 0.15	0.10±0.0
3S-LCA	0	0.08±0.01	0	1.31±0.08
3S-TLCA	0	0	0	1.19±0.19
DCA	0.45 ± 0.02	0.01±0.0	22.14 ± 0.69	11.70±1.8
GDCA	0.46 ± 0.04	0.38±0.03	18.72 ± 1.71	25.10±0.7
TDCA	0	0.39±0.03	0	4.90±0.8

Values are expressed as $\mu\text{g}/10^6$ hepatocytes.

Table 4: In vivo liver damage, Cmax values, tested in vitro concentrations and effects on bile canaliculi deformation of the 10 tested drugs

Drugs	Liver damage	Cmax ($\mu\text{g/mL}$) ²	Tested concentration (μM)	Bile canaliculi deformation
Streptomycin	Non-hepatotoxic	30.4 ^a	2000	No change
Sitaxentan	Hepatocellular injury	22 ^b	50	No change
Acetaminophen	Hepatocellular injury	139 ^c	2000	No change
Amiodarone	Hepatocellular injury	0.8 ^c	10	No change
Ambrisentan	Non-hepatotoxic	2-3.2 ^b	50	No change
Ampicillin	Non-hepatotoxic	6.8 ^d	2000	No change
Troglitazone	Cholestasis	6.39 ^c	10	Constriction
Flucloxacillin	Cholestasis	14.5 ^e	500	Dilatation
Bosentan	Cholestasis	7.4 ^c	10	Dilatation
Perhexilline	Cholestasis ¹	2.16 ^c	10	No change/ Constriction ³
Fasudil	Cholestasis ¹	0.28 ^f	10	Dilatation
Levofloxacin	Cholestasis ¹	0.6-9.4 ^g	50	Dilatation
Erythromycin	Cholestasis	1.4 ^h	10	Dilatation
Macitentan	Cholestasis ¹	0.13-0.75 ^b	10	Dilatation

¹ Rare cases of clinical cholestasis; ² Cmax values are from the literature and refer to the maximum serum concentration of the drug : ^a(Akaho *et al.*, 2002); ^b (Burbank, et al., 2017); ^c(Burbank, et al., 2016); ^d(Wise *et al.*, 1992); ^e(Gardiner *et al.*, 2018); ^f(Fukumoto *et al.*, 2005); ^g(Fish *et al.*, 1997) and ^h(Geerdes-Fenge *et al.*, 1997); ³ BC constriction was observed in some treated cultures.

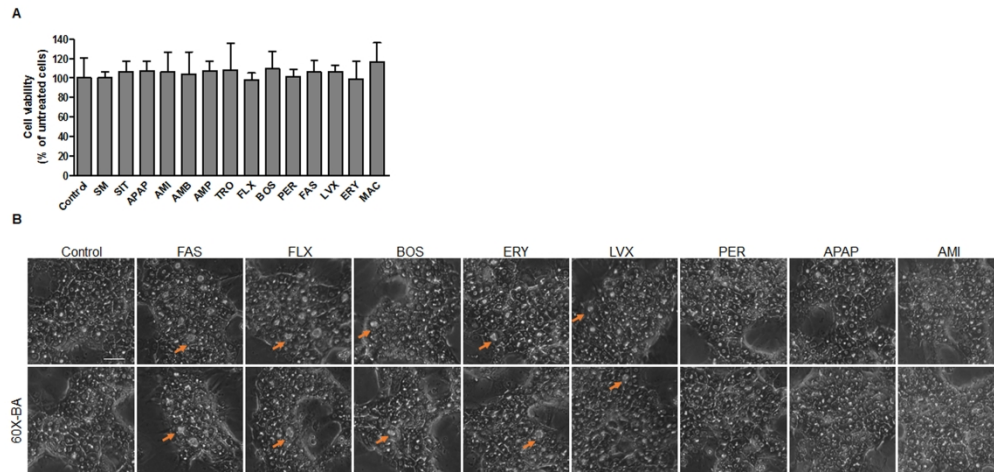


Figure 1. Cytotoxicity and morphological effects of the 60X-BA mixture and tested drugs in human HepaRG cell cultures.

(A) Cytotoxicity of the 60X-BA mixture and tested drugs using the MTT colorimetric assay. HepaRG cells were treated with the 60X-BA mixture alone for 24 h and then with tested drugs combined with BA mixture for additional 24h. Data were expressed relative to those of untreated cells arbitrarily set at 100%. They represent the means \pm S.D of three independent experiments. No significant change was observed. (B) Representative phase-contrast images of HepaRG cells treated with tested drugs alone or in combination with the 60X-BA mixture for 24 h. Images were captured using phase-contrast microscopy (bar = 50 μ m). Orange arrows indicate BC dilatation. No evidence of BC dilatation was observed in cultures treated with PER, APA and AMI.

432x204mm (300 x 300 DPI)

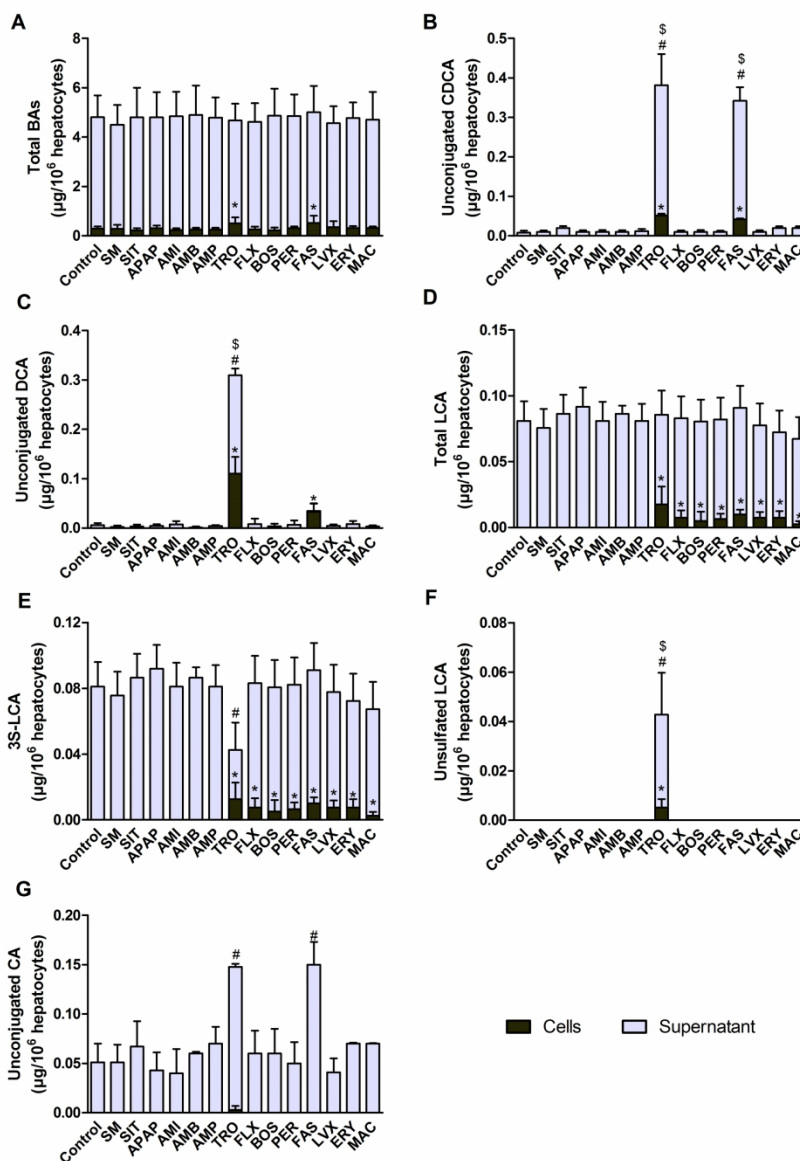


Figure 2. Effects of 24-h treatment with tested drugs on BA profiles in HepaRG cell cultures incubated with the 1X-BA mixture (A) Total BAs; (B) Unconjugated CDCA; (C) Unconjugated DCA; (D) Total LCA; (E) 3S-LCA; (F) Unsulfated LCA and (G) Unconjugated CA in supernatants and cell layers. Both total and individual BAs were calculated in $\mu\text{g}/10^6$ hepatocytes/24 hours. Values represent the mean \pm S.D of three independent experiments. * $P < 0.05$ compared with the values in cell layers of untreated cells; # $P < 0.05$ compared with the values in supernatants of untreated cells; and $\$P < 0.05$ compared with the values in cells + supernatants of untreated cells.

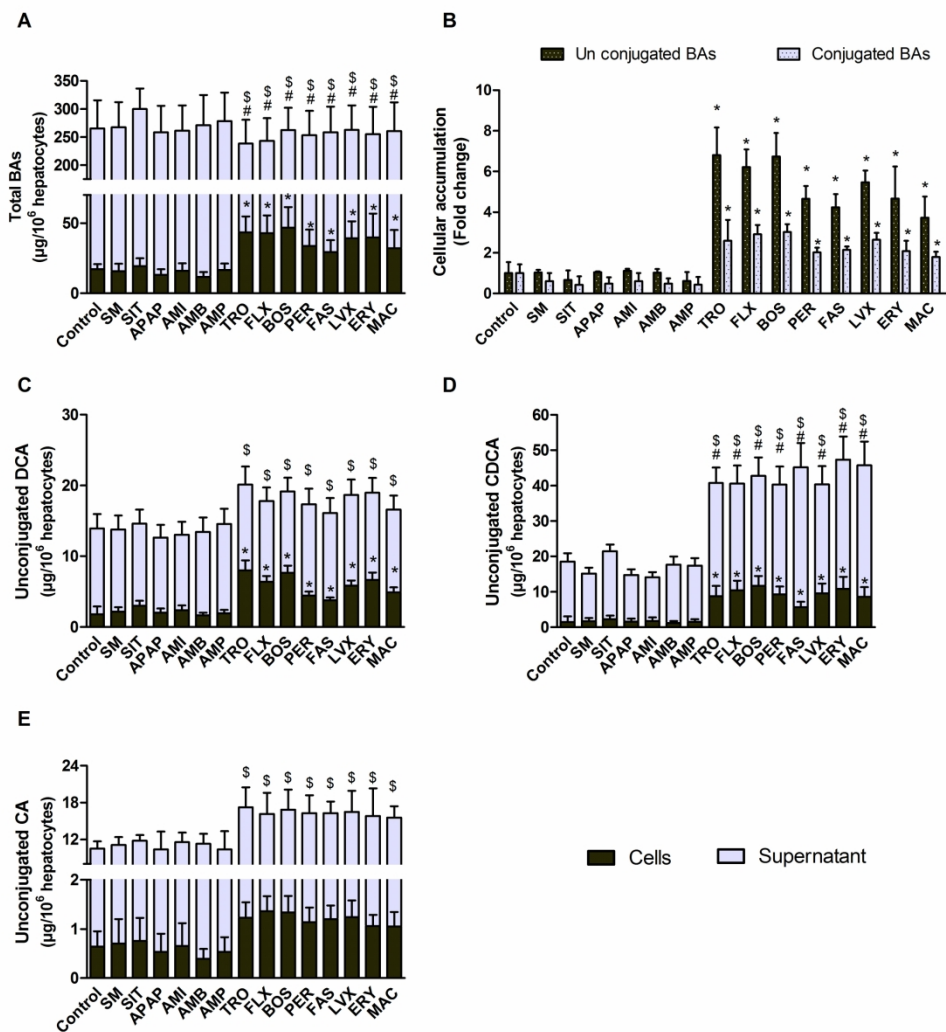


Figure 3. Effects of 24-h treatment with tested drugs on BA profiles in HepaRG cell cultures incubated with the 60X-BA mixture (A) Total BAs; (B) Cellular accumulation of conjugated and unconjugated BAs; (C) Unconjugated DCA and (D) Unconjugated CDCA, in supernatants and cell layers. Both total and individual BAs were calculated in $\mu\text{g}/10^6$ hepatocytes/24 hours. Values represent the mean \pm S.D of three independent experiments. *P < 0.05 compared with the values in cell layers of untreated cells; #P < 0.05 compared with the values in supernatants of untreated cells; and \$P < 0.05 compared with the values in cells + supernatants of untreated cells.

208x223mm (300 x 300 DPI)

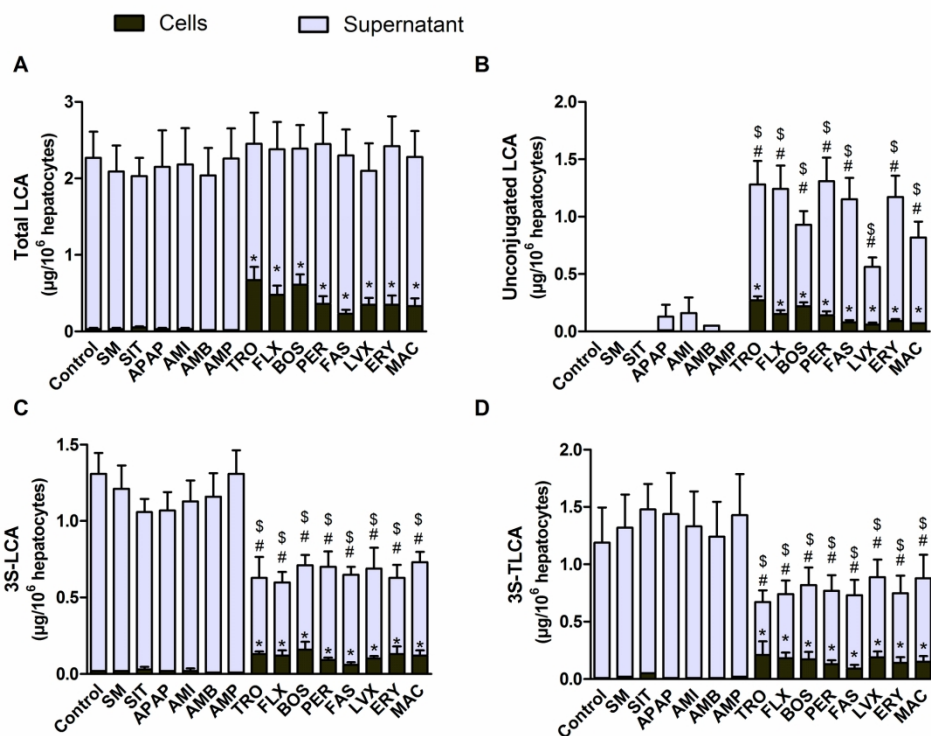


Figure 4. Effects of 24-hour treatment with tested drugs on LCA profiles in HepaRG cell cultures incubated with the 60X-BA mixture (A) Total LCA; (B) Unconjugated LCA; (C) 3S-LCA and (D) 3S-TLCA in cell layers and supernatants. LCA was calculated in $\mu\text{g}/10^6$ hepatocytes/24 hours. Values represent the mean \pm S.D of three independent experiments. * $P < 0.05$ compared with the values in cell layers of untreated cells; # $P < 0.05$ compared with the values in supernatants of untreated cells; and \$ $P < 0.05$ compared with the values in cells + supernatants of untreated cells.

192x150mm (300 x 300 DPI)